Calculating NMR chemical shifts using the augmented plane-wave method

Robert Laskowski
*Institute of High Performance Computing, A*STAR, 1 Fusionopolis Way, #16-16, Connexis, Singapore 138632*

Peter Blaha
Institute of Materials Chemistry, Vienna University of Technology, Getreidemarkt 9/165-TC, A-1060 Vienna, Austria

(Received 28 August 2013; revised manuscript received 20 November 2013; published 6 January 2014)

Density functional theory (DFT) calculations of the magnetic shielding for solid state nuclear magnetic resonance (NMR) provide an important contribution for the understanding of the experimentally observed chemical shifts. Therefore, methods allowing us to compute those parameters with high precision are very valuable. Recently, we have presented a formalism for computing the NMR parameters in solids based on the augmented plane wave (APW) method [Phys. Rev. B **85**, 035132 (2012)]. In the present work we derive an improvement of the original schema, which greatly boosts its precision and efficiency. Although the APW method is virtually an exact method for the ground state wave functions in a solid, its optimized basis set is incomplete and we need to extend it by including basis functions containing the radial derivative of the standard APW basis functions in order to efficiently describe the perturbation due to a magnetic field. In addition we also include the core states in the first-order perturbation formula correcting an error resulting from separation of the core and valence states. These allow us to obtain the NMR parameters that are nearly numerically exact within a given DFT functional.

DOI: 10.1103/PhysRevB.89.014402 PACS number(s): 76.60.Cq, 71.45.Gm, 71.15.−m

I. INTRODUCTION

Solid state nuclear magnetic resonance (NMR) is a powerful and widely used experimental method that provides information about the atomic and electronic structure of materials.[1] It measures the response of a material to an external magnetic field by detecting the transition energies related to the reorientation of the nuclear magnetic moment. The external field induces an electric current in the sample, which according to Biot-Savart's law produces an induced magnetic field that partially screens the external field. The NMR transition energies are proportional to the total magnetic field at the nucleus. The induced current and the corresponding shielding depends strongly on the electronic and atomic structure of the material. In order to interpret the experimental results, it is essential to understand this rather complicated and indirect relation. Density functional theory (DFT) calculations turn out to be extremely helpful for this task. There are, however, several issues that may impact the quality of the calculated parameters. For instance, a rather fundamental problem that concerns the inherent errors of current DFT implementations appears due to the approximate nature of currently used DFT functionals. It manifests itself in the common observation that for a particular nucleus within a series of compounds the comparison of computed shielding parameters with experiment shows some scattering from a straight line, but most severe, also a systematic error resulting in a slope different from 1.0 can appear.[2–8] This issue has been recently discussed by us in Refs. 9 and 10 and the influence of various DFT approximations was demonstrated, but a general solution seems impossible at present and more accurate DFT approximations are needed. Testing of more accurate functionals, however, can be misleading when another, less fundamental problem arise due to limitations and simplifications in the numerical method and the implemented formalism of an NMR shift calculation.

In this paper we modify our previously published formalism[11] to calculate the NMR shielding in solids within the all-electron augmented plane wave (APW) method. This allows us to reach the "DFT limit" and offers a considerable improvement of both computational performance and precision in the calculation of NMR parameters. Moreover, we believe that our conclusions may also be useful for other approaches.

The paper is organized as follows. In the next section we briefly outline the general formalism for computing NMR parameters within the APW method including the extended basis set consisting of many local orbitals (LO) at high energies.[11] In the following section we introduce a more efficient way to deal with the incompleteness of the standard APW basis and also discuss the potential source of errors resulting from the separation of the magnetic response into valence and core state contributions. In the final section we conclude and summarize our findings.

II. THEORETICAL APPROACH: CURRENT STATUS

Until now several methods of *ab initio* calculation of NMR chemical shifts for molecules[12,13] and solids have been described in the literature.[14–18] In the case of solids they usually operate within the standard DFT[19,20] framework, but hybrid DFT has also been used.[9] Our formalism is based on a linear response approach[14,16,21] originally developed by Mauri, Pfrommer, and Louie (MPL),[14] however it is implemented within the all-electron, full potential augmented plane wave method (APW).[22,23] The details of the implementation are described in our previous publication.[11] Formally our method belongs to a set of gauge transformation methods called IGCV (individual gauge for core and valence) with "$d(r) = r$" gauge choice for the valence electrons as elegantly pointed out by Gregor, Mauri, and Car.[24]

The shielding tensor $\overleftrightarrow{\sigma}$ is defined as a proportionality constant between the induced magnetic field $\mathbf{B}_{\rm ind}$ at the nucleus at site $\mathbf{R}$ and the external uniform field $\mathbf{B}$:

$$\mathbf{B}_{\rm ind}(\mathbf{R}) = -\overleftrightarrow{\sigma}(\mathbf{R})\mathbf{B}. \tag{1}$$

Most often only the isotropic shielding (IS) defined as $\sigma(\mathbf{R}) = \mathrm{Tr}[\overleftrightarrow{\sigma}(\mathbf{R})]$ can be accessed experimentally. The actually measured number is the chemical shift δ which is the NMR isotropic shielding obtained with respect to some reference compound $\delta(\mathbf{R}) = \sigma_{\rm ref} - \sigma(\mathbf{R})$.

The induced field $\mathbf{B}_{\rm ind}$ is obtained by integrating the induced current $\mathbf{j}_{\rm ind}(\mathbf{r})$ according to the Biot-Savart law:

$$\mathbf{B}_{\rm ind}(\mathbf{R}) = \frac{1}{c}\int d^3r\ \mathbf{j}_{\rm ind}(\mathbf{r})\frac{\mathbf{R}-\mathbf{r}}{|\mathbf{r}-\mathbf{R}|^3}. \tag{2}$$

For nonmagnetic and insulating materials, only the orbital motion of electrons contribute to $\mathbf{j}_{\rm ind}(\mathbf{r})$. The current density is evaluated as expectation value of the current operator:

$$\mathbf{J}(\mathbf{r}') = -\frac{\mathbf{p}|\mathbf{r}'\rangle\langle\mathbf{r}'| + |\mathbf{r}'\rangle\langle\mathbf{r}'|\mathbf{p}}{2} - \frac{\mathbf{B}\times\mathbf{r}'}{2c}|\mathbf{r}'\rangle\langle\mathbf{r}'|. \tag{3}$$

The expression for the induced current involves only the first-order terms with respect to the external field $\mathbf{B}$:

$$\mathbf{j}_{\rm ind}(\mathbf{r}') = \sum_o \left[\left\langle\Psi_o^{(1)}\middle|\mathbf{J}^{(0)}(\mathbf{r}')\middle|\Psi_o^{(0)}\right\rangle + \left\langle\Psi_o^{(0)}\middle|\mathbf{J}^{(0)}(\mathbf{r}')\middle|\Psi_o^{(1)}\right\rangle + \left\langle\Psi_o^{(0)}\middle|\mathbf{J}^{(1)}(\mathbf{r}')\middle|\Psi_o^{(0)}\right\rangle\right], \tag{4}$$

where $\Psi_o^{(0)}$ is an unperturbed Kohn-Sham (KS) occupied orbital, $J^0(\mathbf{r}')$ is the paramagnetic part of the current operator [the first term in Eq. (3)], and $J^1(\mathbf{r}')$ is the diamagnetic component of the current operator [the second term in Eq. (3)]. $\Psi_o^{(1)}$ is the first-order perturbation of $\Psi_o^{(0)}$ given by the standard formula involving a Greens function:

$$\left|\Psi_o^{(1)}\right\rangle = \sum_e \left|\Psi_e^{(0)}\right\rangle \frac{\left\langle\Psi_e^{(0)}\middle|H^{(1)}\middle|\Psi_o^{(0)}\right\rangle}{\epsilon_o - \epsilon_e}, \tag{5}$$

where $H^{(1)}$ is the perturbation due to the external magnetic field in symmetric gauge:

$$H^{(1)} = \frac{1}{2c}\mathbf{r}\times\mathbf{p}\cdot\mathbf{B}. \tag{6}$$

In the actual implementation the position operator $\mathbf{r}$ is replaced by the limit $\mathbf{r}\cdot\hat{\mathbf{u}}_i = \lim_{q\to 0}\frac{1}{2q}(e^{iq\hat{\mathbf{u}}_i\cdot\mathbf{r}} - e^{-iq\hat{\mathbf{u}}_i\cdot\mathbf{r}})$ to avoid the divergences for extended systems. Moreover Eq. (4) is reformulated using the generalized sum rule[16] in order to remove the dependence on the gauge origin.

In the APW method the unit cell is decomposed into nonoverlapping atomic spheres and an interstitial region. The unperturbed wave functions as well as their first-order perturbations are expressed using plane waves in the interstitial region and an atomiclike angular momentum expansion inside the atomic spheres S_α:

$$\Psi_{n,\mathbf{k}}(\mathbf{r}) = \begin{cases} \frac{1}{\sqrt{\Omega}}\sum_{\mathbf{G}} C_G^{n,\mathbf{k}} e^{i(\mathbf{G}+\mathbf{k})\cdot\mathbf{r}}, & \mathbf{r}\in I, \\ \sum_{lm} W_{lm}^{n,\alpha,\mathbf{k}}(r)Y_{lm}(\hat{r}), & \mathbf{r}\in S_\alpha. \end{cases} \tag{7}$$

The APW basis set inside atomic spheres uses numerical radial functions $W_{lm}^{n,\alpha,\mathbf{k}}(r)$ computed at predefined linearization energies,[22] which are chosen to match the energies of the corresponding occupied bands. Therefore the basis is optimized to describe states with eigenvalues close to the linearization energies. This approach yields basically the exact radial wave functions for all occupied states and shallow conduction states. However, it is not well suited to describe the perturbation of the wave function due to an external magnetic field. Previously we have tried to solve this problem by supplying several additional local orbitals (NMR-LO) with radial wave functions at high energies (up to 1000 Ry) containing 10–20 nodes.[11] This extension is done for all orbital quantum numbers up to $l+1$, where l is the maximal chemically relevant orbital quantum number of the valence states of the specific atom.

III. THEORETICAL APPROACH: IMPROVED SCHEME

A. Augmenting the Greens function with $r\frac{\partial}{\partial r}u$

The extension of the basis with additional NMR-LO functions is very convenient and easy to implement within the APW method, but it is not satisfactory in some cases. Simply due to fact that the radial functions are eigenstates of a spherical Hamiltonian, they are very weakly changing with energy in the region close to the nucleus. Therefore, it turns out to be difficult to converge the computed current in this region with respect to the number of NMR-LO. We propose in this paper a simple and efficient way to overcome this difficulty.

The perturbation Hamiltonian due to the external magnetic field is proportional to a product of position and momentum operators. As a result, the perturbation of the wave function contains component proportional to the derivative of the radial function $[r\frac{\partial}{\partial r}u(r)]$. A direct introduction of basis functions (LOs) based on $r\frac{\partial}{\partial r}u(r)$ is not convenient within the APW formalism, simply because such functions are not eigenstates of the radial Schrödinger equation. Therefore, we propose to add the desired term directly to the Greens function present in the formula for the first-order perturbation of the valence state wave function [Eq. (5)]. The perturbation of any valence wave function can be evaluated by solving Sternheimer equation:

$$(\epsilon_o - H)\left|\Psi_i^{(1)}\right\rangle = \left(1 - \sum_o |\Psi_o\rangle\langle\Psi_o|\right)H^{(1)}|\Psi_i\rangle, \tag{8}$$

where $|\Psi_i^{(1)}\rangle$ can be expanded using the eigenstates of the H:

$$\left|\Psi_i^{(1)}\right\rangle = \sum_j |\Psi_j\rangle\left\langle\Psi_j\middle|\Psi_i^{(1)}\right\rangle. \tag{9}$$

This holds for a complete set of $|\Psi_j\rangle$. Because the APW basis is not complete, we introduce auxiliary functions $|\phi_k\rangle$ that should provide the missing character for the expansion set of $|\Psi_i^{(1)}\rangle$. $|\phi_k\rangle$ are chosen such that $\langle\phi_k|\Psi_j\rangle = 0$ for any $|\Psi_j\rangle$ and $\langle\phi_i|\phi_j\rangle = 0$ for $i\neq j$. Augmented expansion of $|\Psi_i^{(1)}\rangle$ will have a following form:

$$\left|\Psi_i^{(1)}\right\rangle = \sum_j |\Psi_j\rangle\left\langle\Psi_j\middle|\Psi_i^{(1)}\right\rangle + \sum_k |\phi_k\rangle\left\langle\phi_k\middle|\Psi_i^{(1)}\right\rangle. \tag{10}$$

The expansion coefficient $\langle\phi|\Psi_i^{(1)}\rangle$ is simply evaluated with

$$\left\langle\phi_k\middle|\Psi_i^{(1)}\right\rangle = \frac{\langle\phi_k|H^1|\Psi_i\rangle}{\langle\phi_k|(\epsilon_i - H)|\phi_k\rangle}. \tag{11}$$

This can be equivalently formulated as in Eq. (5):

$$\left|\Psi_i^{(1)}\right\rangle = \mathcal{G}(\epsilon_i)H^{(1)}|\Psi_i\rangle, \tag{12}$$

where

$$\mathcal{G}(\epsilon_i) = \sum_e \frac{\left|\Psi_e^{(0)}\right\rangle\left\langle\Psi_e^{(0)}\right|}{\epsilon_i - \epsilon_e} + \sum_k \frac{|\phi_k\rangle\langle\phi_k|}{\langle\phi_k|(\epsilon_i - H)|\phi_k\rangle}. \tag{13}$$

The auxiliary functions $|\phi_k\rangle$ are zero in the interstitial region, and inside the atomic spheres they take an usual APW form: $|\phi_{lm,k}\rangle = \tilde{u}_{l,k}(r)Y_{lm}$. The functions $\tilde{u}_{l,k}(r)$ are constructed by orthogonalizing a function $\xi_{l,k}(r,\tilde{\epsilon})$ to all $u_{l,i}(r)$ present in the APW basis set. Namely, $\tilde{u}_{l,k}(r) = \xi_{l,k}(r,\tilde{\epsilon}) - \sum_i b_{l,k,i}u_{l,i}(r)$, where the parameters $b_{l,k,i}$ are chosen such that $\langle\tilde{u}_{l,k}(r)|u_{l,i}(r)\rangle = 0$ for each radial function $u_{l,i}(r)$. The function $\xi_{l,k}(r,\tilde{\epsilon})$ is chosen such that the product $\xi_{l,k}(r)Y_{lm}$ resembles the effect of $r\nabla_i[u_l(r)Y_{lm}]$. Therefore, we use two $\tilde{u}_{l,k}$ and $\xi_{l,k}(r)$ functions for each $l > 0$ ($k = 1,2$), and only one for $l = 0$ ($k = 1$):

$$\xi_{l,k}(r,\tilde{\epsilon}) = \begin{cases} r\frac{d}{dr}u_{l+1}(r,\tilde{\epsilon}) + (l+2)u_{l+1}(r,\tilde{\epsilon}), & k = 1, \\ r\frac{d}{dr}u_{l-1}(r,\tilde{\epsilon}) - (l-1)u_{l-1}(r,\tilde{\epsilon}), & k = 2. \end{cases} \tag{14}$$

In addition, for $l > 0$ the two $\tilde{u}_{l,k}$ are orthogonalized to each other. Our test shows that the energy $\tilde{\epsilon}$ can be freely chosen within the valence band and the results do not depend on this choice. In the following discussion we will use the acronym "DUC," which means that the standard APW radial basis functions $u_l(r)$ have been enhanced by different radial functions as defined above, when referring to this method.

B. Correction of the effect of core/valence separation

Another issue that may impact the computed current is related to the common approximation, in which the response from core and valence bands is computed separately.[24] In our APW implementation, and possibly in others DFT codes, all states that fall below a certain threshold (in our case -7 Ry) are well localized and treated as core states. The core eigenvalues and their radial functions are obtained as the solution of the radial Dirac equation using the spherical part of the self-consistent potential within the atomic spheres. Subsequently, the core state contribution to the induced current is computed using the spherical symmetric core density only:

$$\mathbf{j}_{\text{ind}}(\mathbf{r}') = -\frac{1}{2c}\rho_{\text{core}}(\mathbf{r}')\mathbf{B}\times\mathbf{r}', \tag{15}$$

and at the same time the expression in Eq. (5) involves only the sum over unoccupied states. However, Eq. (5) is formally correct only when all occupied states (including the core) are included in the sum in Eq. (4) for the expectation value of the current. Otherwise a sizable error may appear. In order to correct this error we include the core states into the first-order perturbation formula in Eq. (5), as suggested by Gregor, Mauri, and Car[24]:

$$\left|\Psi_o^{(1)}\right\rangle = \sum_e \left|\Psi_e^{(0)}\right\rangle \frac{\left\langle\Psi_e^{(0)}\right|H^{(1)}\left|\Psi_o^{(0)}\right\rangle}{\epsilon_o - \epsilon_e} + \sum_{\text{core}} \left|\Psi_{\text{core}}^{(0)}\right\rangle \frac{\left\langle\Psi_{\text{core}}^{(0)}\right|H^{(1)}\left|\Psi_o^{(0)}\right\rangle}{\epsilon_o - \epsilon_{\text{core}}}, \tag{16}$$

where the second term is the core related correction. In further discussion when referring to the effect of this core correction term we will use the acronym "CC." In our APW implementation the valence states are computed within a scalar relativistic approximation,[25] but the core states are the solutions of the Dirac equation with the spherical part of the potential. These different approaches result in a tiny nonorthogonality between core and valence states. Our tests show that even for heavy atoms like Xe the error introduced to the induced current is very small and localized in a region very close to the nucleus (<0.02 a.u.), leading to an error in the calculated σ of less than 0.2 ppm.

Gregor, Mauri, and Car[24] showed that for molecules and Gaussian basis sets the contribution to the absolute chemical shift of a selected atom due to the core-valence transition term does not depend on the chemical environment. In the following we show the effect for selected solids, and also discuss the error introduced in the induced current when this term is neglected.

IV. RESULTS AND DISCUSSION

A simple way to test the accuracy of our formalism is to compare the induced current and absolute shielding calculated for an isolated atom where the correct values can be obtained using the formula

$$\mathbf{j}_\rho(\mathbf{r}') = -\frac{1}{2c}\rho(\mathbf{r}')\mathbf{B}\times\mathbf{r}', \tag{17}$$

which is exact for spherically symmetric charge densities $\rho(\mathbf{r}')$. Because $\rho(\mathbf{r}')$ can be easily computed with high precision, it is easy to reach the (numerically) exact DFT solution $\mathbf{j}_\rho(\mathbf{r}')$, which can serve as a reference for any other method. As a test example we use an Ar atom put into a cubic face-centered box with 50 a.u. lattice size. The standard computational parameters used in WIEN2k already lead to fairly well converged results, but in order to ensure full convergence, the plane wave cutoff was set to a large value of $R_{\text{min}}K_{\text{max}} = 9$, where R_{min} is the smallest sphere radii in the system and K_{max} is the plane wave momentum cutoff. The Brillouin zone was sampled with the Γ point only. The calculations have been performed using the scalar relativistic approximation[25] for valence electrons (eigenstates above -7 Ry) and the fully relativistic Dirac equation was used for core electrons (below -7 Ry). The DFT exchange correlation functional is set to the standard Perdew, Burke, Ernzerhof (PBE) version of the generalized gradient approximation.[26]

Figure 1 shows the induced current as a function of distance from the nucleus (R) calculated with/without DUC and CC and compared to j_ρ computed using Eq. (17). The number of NMR-LO functions[11] was set to 10 in order to reduce the effect of the DUC as much as possible. For clarity only contributions from the top most valence states ($3s$ and $3p$) are shown. We can see that the computed j_{ind} without CC and DUC deviates from the exact j_ρ as far as 0.5 a.u. from the nucleus. Including CC (but not yet DUC) decreases this range to roughly 0.25 a.u. When both DUC and CC are used, j_{ind} matches nearly perfectly j_ρ. The resulting absolute shielding is displayed in Fig. 2 as a function of the number of additional NMR-LOs (see Sec. II). First, we notice that when both DUC and CC are switched off, the calculated σ (blue line in Fig. 2) converges rather

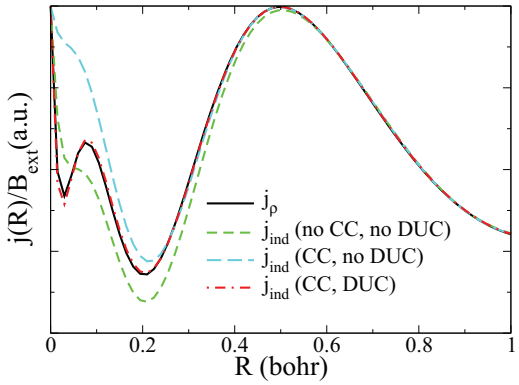

FIG. 1. (Color online) Comparison of the induced current computed for an Ar atom with and without DUC and CC corrections (see text). For clarity only the valence $3s$ and $3p$ contribution is shown. j_ρ is the diamagnetic current calculated with the spherical charge density of $3s$ and $3p$ states using Eq. (17).

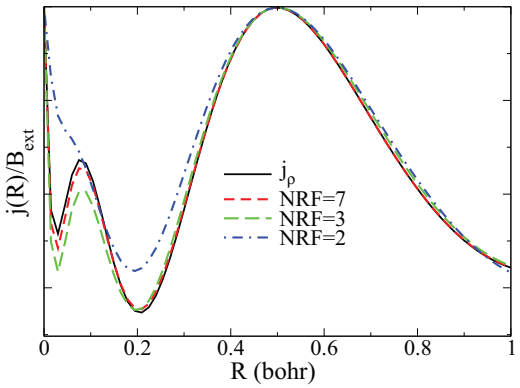

FIG. 3. (Color online) Convergence of the valence current ($3s$ and $3p$ states) in Ar with respect to the number of NMR-LO functions in our APW basis (NRF). DUC and CC corrections have been included in the calculations. j_ρ is the current computed from Eq. (17).

slowly with the number of NMR-LOs and in addition even the extrapolated value would not agree with the correct results (σ_{Ar}), because the CC term is missing. On the other hand, we see that the effects due to DUC and CC are fairly independent of each other. The CC contribution is rather independent on the number of NMR-LOs and results in a fairly constant 8 ppm downward shift compared to the uncorrected values. As expected, the DUC greatly improves the convergence of the calculated σ with respect to the number of NMR-LOs because it introduces radial functions with correct shape into our APW basis. Contrary to CC, DUC results in an upward correction of the shielding and the size of the correction depends on the number of NMR-LO functions in the basis set. Interestingly, DUC and CC seem to partially compensate each other, such that for a moderate number of NMR-LO (8 in this particular case) the results computed without DUC and CC corrections are closer to the exact value $\sigma_{\mathrm{Ar}} = 1245.7$ ppm than when only one of the two corrections is included (see blue line in Fig. 2). Apparently, the agreement in this case is a result of an error cancellation and the computed current differs significantly from the true j_ρ near the nucleus, as seen in Fig. 1. The convergence of the induced current with respect to the number of NMR-LOs when both DUC and CC corrections are included is shown in Fig. 3. Basically three NMR-LOs are sufficient to reproduce the shape of the exact j_ρ.

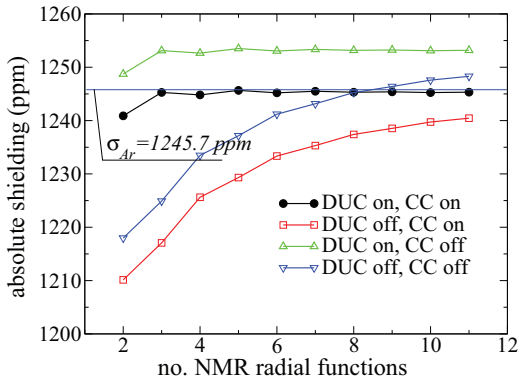

FIG. 2. (Color online) Convergence of NMR absolute shieldings σ of an Ar atom with respect to the number of NMR-LO in the APW basis and with/without DUC and CC correction. The vertical blue line represents the value of the absolute shielding $\sigma_{\mathrm{Ar}} = 1245.7$ ppm computed using j_ρ from Eq. (17) and integrated according to Eq. (2).

We have performed similar analysis also for He, Ne, Kr, and Xe atoms. In all cases the computed values of the absolute NMR shielding using the perturbation approach did not differ mere than 0.5 ppm from the exact σ calculated using the charge density formula [Eq. (17)].

Another stringent test of the quality of our results concerns the generalized f-sum rule,[16] which proves that the basis set is complete. We have integrated the f-sum rule with respect to $\mathbf{r}$ and checked the resulting number of electrons. For all cases mentioned above (He, Ne, Ar, Kr, and Xe), but also for molecules like SiF_4 or $CFCl_3$, which are simulated in a big box, this test is fulfilled within 0.1% (or better) and can be considered as virtually exact. If we omit the DUC extension of our basis, the sum rule has errors up to 2% (depending on the number of NMR-LOs), which is similar to the best Gaussian basis sets used in Ref. 24 for molecules containing second row elements.

Recently in Ref. 9 we have published computed shielding parameters for a series of fluorides, oxides, chlorides, and bromides. The discussion in Ref. 9 focused mainly on the origin of the systematic error, which is present in DFT calculations of the NMR shielding and manifests itself in the slope of the experiment vs theory relation. These slopes, which must have a value of -1.0, range from -0.8 to -1.25, depending on the specific DFT functional. Table I presents the revised NMR shielding parameters computed using the PBE exchange correlation functional including both CC and DUC. When comparing these new results to the ones from Ref. 9, the correction due to DUC depends in general on the quality of the previously used basis set, especially on the number of NMR-LOs and thus varies from case to case.

The effect of CC is, however, fairly independent not only on the basis size but also on the chemical composition as indicated in Table I. The contribution due to the CC term for fluorides range between 20 and 21 ppm, which is nearly equal to the number quoted by Gregor, Mauri, and Car[24] for a series of F

TABLE I. The isotropic shielding σ_{iso} computed including both DUC and CC, correction due to CC ($\sigma_{iso} - \sigma_{iso}^{nocc}$) calculated for ^{19}F in fluorides, ^{17}O in oxides, $^{35-37}$Cl in chlorides, and $^{79-81}$Br in bromides. We compare our results with available measured NMR chemical shifts. The experimental shifts $\delta_{iso}^{expt.}$ are given with reference to $CFCl_3$ for ^{19}F, H_2O for ^{17}O, KBr for $^{79-81}$Br, and 1 M NaCl(aq) for $^{35-37}$Cl. The theoretical shifts δ_{iso} are given using a reference taken from an unconstrained (slope different from -1) linear fit of the calculated absolute shieldings vs experimental shifts for each compound series. All values in ppm. Columns χ_m and χ_m (expt.) show calculated and measured[27–29] susceptibilities given in units of 10^{-6} cm^3 mol^{-1}.

	Space group	σ_{iso}	$\sigma_{iso} - \sigma_{iso}^{nocc}$	δ_{iso}	δ_{iso} (expt.) [Ref.]	χ_m	χ_m (expt.)
Fluorides							
LiF	Fm-$3m$	369.91	−20.39	−205.4	−204.3[4]	−10.8	−10.1
NaF	Fm-$3m$	394.72	−20.13	−224.9	−224.2[4]	−17.6	−15.6
KF	Fm-$3m$	270.83	−20.32	−127.4	−133.3[4]	−23.4	−23.6
RbF	Fm-$3m$	223.16	−20.26	−90.0	−90.9[4]	−31.5	−31.9
CsF	Fm-$3m$	126.73	−20.33	−14.1	−11.2[4]	−44.3	−44.5
MgF_2	$P42/mnm$	362.87	−20.33	−199.8	−197.3[4]	−23.5	−22.7
CaF2	Fm-$3m$	220.56	−20.32	−87.9	−108.0[4]	−25.8	−28
SrF_2	Fm-$3m$	215.97	−20.37	−84.3	−87.5[4]	−34.4	−37.2
BaF_2	Fm-$3m$	125.81	−20.39	−13.4	−14.3[4]	−44.8	−51
α-AlF3	R-$3c$	335.68	−20.36	−178.4	−172.0[30]	−15.2	−13.9
GaF_3	R-$3c$	323.53	−20.60	−168.9	−171.2[31]	−42.0	
InF3	R-$3c$	383.90	−20.97	−216.4	−209.2[31]	−55.5	
TlF	$Pbcm$	149.16	−21.68	−31.8	−19.1[32]	−51.4	−44.4
Oxides							
BeO	$P63mc$	234.20	−14.71	21.1	26[33]	−12.6	−11.9
MgO	Fm-$3m$	200.40	−13.71	49.8	47[33]	−15.8	−10.2
CaO	Fm-$3m$	−145.53	−14.17	343.4	294[2]	−11.4	−15.0
SrO	Fm-$3m$	−217.04	−14.19	404.1	390[33]	−16.5	−35
BaO	Fm-$3m$	−481.50	−14.17	628.6	629[33]	−17.3	−29.1
SiO_2	$P3221$	244.28	−14.49	12.5	41[34]	−24.8	−28.6
$SrTiO_3$	Pm-$3m$	−290.24	−14.29	466.3	465[35]	−10.1	
$BaZrO_3$	Pm-$3m$	−174.53	−14.32	368.1	376[35]	−39.3	
$BaSnO_3$	Pm-$3m$	86.23	−14.96	146.7	143[3]	−73.3	
$BaTiO_3$	$P4mm$	−366.79	−14.32	531.2	564[3]	−12.6	
		−361.04	−14.34	526.4	523[3]		
Chlorides							
LiCl	Fm-$3m$	919.01	−5.46	−0.5	5.0[36,37]	−11.2	−10.8
NaCl	Fm-$3m$	978.87	−5.79	−49.6	−47.4[36,37]	−31.8	−30.2
KCl	Fm-$3m$	912.28	−5.76	5.0	3.1[36,37]	−39.6	−38.8
RbCl	Fm-$3m$	868.02	−5.75	41.3	43.2[36,37]	−46.8	−46
CsCl	Pm-$3m$	789.54	−5.73	105.7	110[36,37]	−59.2	−56.7
AgCl	Fm-$3m$	901.19	−5.39	14.1	9.8[37,38]	−48.3	−49
TlCl	Pm-$3m$	618.23	−6.96	246.3	250.5[37]	−62.0	−57.8
$CaCl_2$	$Pnnm$	755.20	−5.67	133.9	122[37,39]	−50.2	−54.7
$SrCl_2$	Fm-$3m$	746.43	−5.80	141.1	140.8[36,37]	−58.4	−61.5
$BaCl_2$	$Pnma$	767.62	−5.77	123.7	124[37,40]	−68.0	−72.6
		651.27	−5.84	219.2	219[37,40]		
Bromides							
LiBr	Fm-$3m$	2573.80	−313.45	60.4	64.7[37,41]	−35.9	−34.3
NaBr	Fm-$3m$	2729.36	−313.37	−53.9	−52.9[37,41]	−43.1	−41
KBr	Fm-$3m$	2651.68	−313.31	3.2	0[37,41]	−51.0	−49.1
RbBr	Fm-$3m$	2571.54	−313.31	62.1	71.7[37,41]	−58.7	−56.4
CsBr	Pm-$3m$	2359.51	−313.70	217.9	227.4[37,41]	−74.5	−67.2
AgBr	Fm-$3m$	2406.08	−313.53	183.7	169.3[37,41]	−55.8	−61
$CaBr_2$	$Pnnm$	2232.77	−313.39	311.1	280[7]	−72.9	−73.8
$SrBr_2$	$P4/nz$	2110.51	−315.47	401.0	422[7]	−81.8	−86.6
		2135.72	−315.48	382.4	410[7]		
		2238.42	−315.48	306.9	320[7]		
		2253.45	−315.48	295.9	300[7]		
$BaBr_2$		2236.40	−313.48	308.4	280[7]	−71.6	−92
		2023.26	−313.45	465.1	480[7]		
TlBr	Pm-$3m$	1801.88	−314.64	627.8	600[37,42]	−70.1	−63.9

containing molecules. The correction for oxides and chlorides oscillates around 13–14 ppm and 5–6 ppm, respectively. The large CC correction of 313–315 ppm for bromides is due to Br-3*d* states, which are included as valence states in our calculations.

In summary, the relation between experimental and theoretical shifts are not changed at all compared to our previous results and all conclusions and trends presented in Ref. 9 are still valid.

The magnetic susceptibility χ_m determines the macroscopic component of the induced magnetic filed,[16] which may result into a contribution of several ppm to the shielding, therefore we have included the computed χ_m in Table I and compare it to the measured values. For fluorides, oxides, and chlorides the DUC and CC corrections have only a minor effect on χ_m. For bromides, however, due to the presence of Br-3*d* states in the valence panel, CC may correct χ_m by as much as 20%. Except for some oxides like SrO and BaO the the computed values compare quite well with the measured values.[27–29]

V. CONCLUSIONS

In this paper we have demonstrated that our revised formalism provides a very precise method for computing the NMR shielding parameters within DFT. For the test cases, the difference between the results computed with the first-order perturbation approach and the (numerically) exact atomic values computed using spherically symmetric charge densities, are below 0.5 ppm. Moreover, our method is able to reproduce not only the value of the absolute shielding but also captures correctly the shape of the induced current, including its oscillatory character near the nucleus. The CC correction arising due to the separation of the core and valence states is independent on the APW basis extension and fairly constant within a given series. The DUC correction on the other hand, greatly improves the convergence with respect to the number of NMR-LOs, which leads to a substantial improvement in the performance of the calculations. While we are now able to reach the DFT limit when calculating absolute NMR shifts, it seems that when we compare the revised data calculated for the series of fluorides, oxides, chlorides, and bromides the corrections resulted mainly in a rigid shift of the computed absolute isotropic shielding and do not change any previous results qualitatively.

ACKNOWLEDGMENTS

We would like to acknowledge support by the Austrian Science Foundation (FWF) in project SFB-F41 (ViCoM). This work was supported by the A*STAR Computational Resource Centre through the use of its high performance computing facilities.

[1] C. M. Grant and R. K. Harris (Eds.), *Encyclopedia of NMR* (Wiley, New York, 1996).
[2] M. Profeta, M. Benoit, F. Mauri, and C. J. Pickard, J. Am. Chem. Soc. **126**, 12628 (2004).
[3] D. S. Middlemiss, F. Blanc, C. J. Pickard, and C. P. Grey, J. Magn. Reson. **204**, 1 (2010).
[4] A. Sadoc, M. Body, C. Legein, M. Biswal, F. Fayon, X. Rocquefelte, and F. Boucher, Phys. Chem. Chem. Phys. **13**, 18539 (2011).
[5] C. M. Widdifield and D. L. Bryce, J. Phys. Chem. A **114**, 10810 (2010).
[6] M. Kibalchenko, J. R. Yates, C. Massobrio, and A. Pasquarello, Phys. Rev. B **82**, 020202 (2010).
[7] C. M. Widdifield and D. L. Bryce, J. Phys. Chem. A **114**, 2102 (2010).
[8] C. Bonhomme, C. Gervais, N. Folliet, F. Pourpoint, C. Coelho Diogo, J. Lao, E. Jallot, J. Lacroix, J.-M. Nedelec, D. Iuga *et al.*, J. Am. Chem. Soc. **134**, 12611 (2012).
[9] R. Laskowski, P. Blaha, and F. Tran, Phys. Rev. B **87**, 195130 (2013).
[10] R. Laskowski and P. Blaha, Phys. Rev. B **85**, 245117 (2012).
[11] R. Laskowski and P. Blaha, Phys. Rev. B **85**, 035132 (2012).
[12] T. Helgaker, M. Jaszunski, and K. Ruud, Chem. Rev. **99**, 293 (1999).
[13] M. Kaupp, B. M., and V. G. Malkin (Eds.), *Calculation of NMR and EPR Parameters. Theory and Applications* (Wiley, New York, 2004).
[14] F. Mauri, B. G. Pfrommer, and S. G. Louie, Phys. Rev. Lett. **77**, 5300 (1996).
[15] D. Sebastiani and M. Parrinello, J. Phys. Chem. A **105**, 1951 (2001).
[16] C. J. Pickard and F. Mauri, Phys. Rev. B **63**, 245101 (2001).
[17] T. Thonhauser, D. Ceresoli, A. A. Mostofi, N. Marzari, R. Resta, and D. Vanderbilt, J. Chem. Phys. **131**, 101101 (2009).
[18] D. Skachkov, M. Krykunov, and T. Ziegler, Can. J. Chem. **89**, 1150 (2011).
[19] P. Hohenberg and W. Kohn, Phys. Rev. **136**, B864 (1964).
[20] W. Kohn and L. J. Sham, Phys. Rev. **140**, A1133 (1965).
[21] J. R. Yates, C. J. Pickard, and F. Mauri, Phys. Rev. B **76**, 024401 (2007).
[22] D. J. Singh and L. Nordström, *Planewaves, Pseudopotentials and the LAPW Method*, 2nd ed. (Springer, New York, 2006).
[23] P. Blaha, K. Schwarz, G. K. H. Madsen, D. Kvasnicka, and J. Luitz, *WIEN2k, An Augmented Plane Wave Plus Local Orbitals Program for Calculating Crystal Properties* (Vienna University of Technology, Austria, 2001).
[24] T. Gregor, F. Mauri, and R. Car, J. Phys. Chem. **111**, 1815 (1999).
[25] D. D. Koelling and B. N. Harmon, J. Phys. C **10**, 3107 (1977).
[26] J. P. Perdew, K. Burke, and M. Ernzerhof, Phys. Rev. Lett. **77**, 3865 (1996).
[27] *Landolt-Bornstein, Numerical Data and Functional Relationships in Science and Technology, New Series, II/16, Diamagnetic Susceptibility* (Springer, Heidelberg, 1986).
[28] *Landolt-Bornstein, Numerical Data and Functional Relationships in Science and Technology, New Series, II/2, II/8, II/10, II/11, and II/12a, Coordination and Organometallic Transition Metal Compounds* (Springer, Heidelberg, 1966–1984).
[29] *Tables de Constantes et Donnes Numrique, Volume 7, Relaxation Paramagnetique* (Masson, Paris, 1957).
[30] P. J. Chupas, M. F. Ciraolo, J. C. Hanson, and C. P. Grey, J. Am. Chem. Soc. **123**, 1694 (2001).

[31]B. Bureau, G. Silly, J. Buzaré, and J. Emery, Chem. Phys. **249**, 89 (1999).
[32]S. Gabuda, S. Kozlova, and R. Davidovich, Chem. Phys. Lett. **263**, 253 (1996).
[33]G. L. Turner, S. E. Chung, and E. Oldfield, J. Magn. Reson. **64**, 316 (1985).
[34]M. Profeta, F. Mauri, and C. J. Pickard, J. Am. Chem. Soc. **125**, 541 (2003).
[35]T. J. Bastow, P. J. Dirken, M. E. Smith, and H. J. Whitfield, J. Phys. Chem. **100**, 18539 (1996).
[36]F. Lefebvre, J. Chim. Phys. **89**, 1767 (1992).
[37]C. M. Widdifield, R. P. Chapman, and D. L. Bryce, Annu. Rep. NMR Spectrosc. **66**, 195 (2009).
[38]S. Hayashi and K. Hayamizu, J. Phys. Chem. Solids **53**, 239 (1992).
[39]T. O. Sandland, L.-S. Du, J. F. Stebbins, and J. D. Webster, Geochim. Cosmochim. Acta **68**, 5059 (2004).
[40]J. F. Stebbins and L. S. Du, Am. Mineral. **87**, 359 (2002).
[41]S. Hayashi and K. Hayamizu, Bull. Chem. Soc. Jpn. **63**, 913 (1990).
[42]T. Kanada, J. Phys. Soc. Jpn. **10**, 85 (1955).